Experimental study of two-dimensional electron vortex dynamics in an applied irrotational shear flow

D. L. Eggleston
Department of Physics, Occidental College, Los Angeles, California 90041

(Received 10 August 1994; accepted 9 September 1994)

An electron column in a modified Malmberg–Penning trap is used to study the behavior of a single two-dimensional vortex in an imposed irrotational shear flow. Phosphor screen images are presented, showing the dispersion of a vortex in a strong shear flow. The images show a variety of phenomena, including the fission of the original vortex, the emission, stretching, and entrainment of filamentary arms, and turbulent diffusion. The vortex lifetime is measured as a function of applied shear, with vortex strength independently adjustable. These data are compared to the predictions of a fluid theory, which correctly identifies the key dimensionless parameter (shear rate/vorticity), but not its critical value. The experimental lifetime of a vortex in a strong shear is found to be the same as the dispersion time of a patch of zero vorticity. The lifetime of an unsheared vortex appears to be limited by a slow diffusion that gradually weakens the vortex. © *1994 American Institute of Physics.*

I. INTRODUCTION

Although fluid vortices have been studied for well over a hundred years, they continue to be the subject of active research, receiving an impetus from a number of problems in pure and applied physics.[1] A basic issue in vortex dynamics concerns the fate of a two-dimensional (2-D) vortex in a shear flow (plane strain). The interaction can be described as a competition between the shearing flow, which tries to disperse the vortex, and the vortical motion, which tries to maintain the vortex. Moore and Saffman[2] studied this problem analytically, and found that an elliptical vortex patch (i.e., a region of constant vorticity bounded by an ellipse) could exist in an irrotational shear flow, only if the strain rate was less than a critical value. Kida[3] later showed that when the strain rate exceeded this value, the ellipse would undergo irreversible elongation, and thus the vortex would be dispersed.

The work of Moore and Saffman and Kida is based on the classical theory of inviscid, constant density fluids, as modeled by the Euler equations. As noted recently by Driscoll and Fine,[4] such work can be applied directly to strongly magnetized pure electron plasmas, since the two-dimensional drift-Poisson equations describing such plasmas are isomorphic to the Euler equations. In the plasma system, the vorticity (a key fluid quantity) is proportional to the electron density, which is easily measured, and the viscosity and boundary drag are very small. These features make such systems ideal for testing 2-D vortex theory.[5] For example, Fine *et al.*[6] have used such a system to study symmetric vortex merger.

In this paper an electron column system is used to study the behavior of a single 2-D vortex in an imposed irrotational shear flow. Phosphor screen images are presented, which show the qualitative evolution of a vortex in a strong shear flow. The evolution is characterized by the emission of filamentary arms, and sometimes by the fission of the original vortex. The vortex lifetime is measured as a function of applied shear, with vortex strength independently adjustable, and compared to the prediction of the theory of Moore and Saffman. Consistent with the theory, the vortex lifetime increases significantly when the applied shear is less than a critical value. For subcritical shear values, the vortex lifetime appears to be limited by a slow diffusion, which gradually weakens the vortex.

II. EXPERIMENTAL DEVICE

The apparatus used in these experiments, shown schematically in Fig. 1, is a modified Malmberg–Penning trap.[7] A long conducting cylinder is divided axially into eight electrically isolated parts, labeled G1, S1, S2, S3, S4, S5, G2, and G3. Each of these cylinders is 6.0 in. long, has an I.D. of 3.05 in., and is separated from the others by a gap of 0.050 in. Two of the cylinders (G1 and G2) act as gates for the trap, while the others are normally grounded and provide a well-defined boundary condition for the trapped electrons. Each of the cylinders S1–S5 is divided azimuthally into eight sections, which can be used to monitor the azimuthal motion of the electrons. The apparatus is placed in a vacuum of $<10^{-9}$ Torr, and is immersed in a uniform axial magnetic field produced by a large solenoid. For these experiments $B = 500$ G. At this magnetic field strength, the Larmor radius is less than 0.1 mm and the electron dynamics are well described by the $\mathbf{E}\times\mathbf{B}$ drift motion.

The above description is fairly common for Malmberg–Penning traps. Some distinctive features of this apparatus are as follows: The electrons are produced by a small diameter (0.1 in.) oxide-coated cathode that is placed off axis ($r = 1.55$ cm). This is used to inject a column of electrons into the system. The column's self-field causes it to spin around its axis (i.e., it forms a vortex). A long, thin (0.014 in. diam), conducting wire runs along the axis of the device, and can be biased by the operator. This is used to produce a radial electric field, and thus an azimuthal $\mathbf{E}\times\mathbf{B}$ drift velocity, which is a function of radius and has zero curl (i.e., an irrotational shear flow). The voltage placed on the central wire of the device can be either negative or positive, and thus the ap-

 1070-664X/94/1(12)/3850/7/$6.00

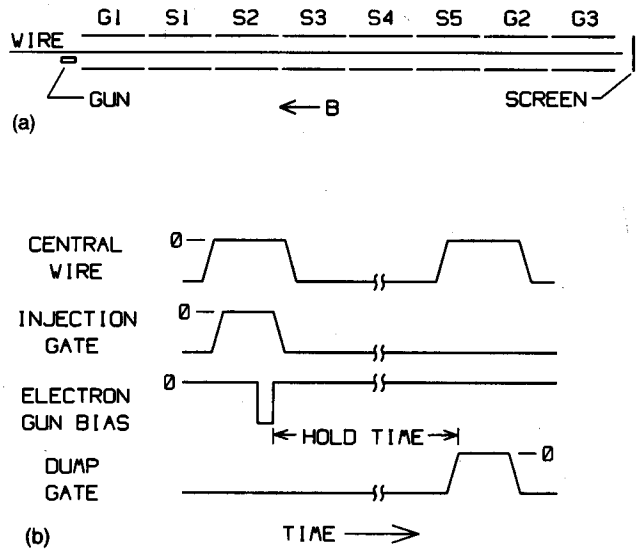

FIG. 1. Experimental device and timing sequence. (a) Schematic of experimental apparatus. (b) Timing diagram for one cycle of the experiment. Voltages applied to the central wire, injection gate (G1), electron gun, and dump gate (G2) are shown.

plied shear flow can either oppose the vortex rotation (adverse shear) or favor it (favorable or prograde shear). Finally, a phosphor-coated screen is used to measure the total charge of the dumped electrons and to produce an image that shows the position and density of the electrons. The images are acquired with a CCD camera and stored and analyzed with a computer-controlled frame grabber.

The apparatus is run in cycles, as shown in Fig. 1(b). To start a cycle, the central wire bias and injection gate bias are switched to zero and a negative pulse is applied to the electron gun. This allows an off-axis column of electrons to fill the device. The density of the electrons can be adjusted by changing the gun bias. The injection gate is then returned to a negative bias, which traps the electrons between G1 and G2. The central wire bias is then switched to a selected value, thus producing a shear flow. After a time selected by the operator, the central wire and the gate G2 are grounded, allowing the electrons to stream out of the device along magnetic field lines and be collected by the positively biased phosphor screen. The total charge in the machine at the time of the dump is thus obtained, as well as an axially integrated image of the electron positions. Typically, several cycles are required to produce enough light for a visable image. On subsequent cycles the hold time can be varied, so that a sequence of images representing the time evolution of the vortex is produced. The shot-to-shot variation in the injected vortex is small enough that each shot evolves identically for 20–80 μs, after which shot-to-shot variations in the dump-time position of the vortex cause a smearing of the multi-cycle image. After this point, one or more of the azimuthal sectors of cylinders S1–S5 can be used to monitor the azimuthal motion of the vortex. This is done by attaching the sector to ground through a resistor, and observing the voltage fluctuations across the resistor produced by the variations in the vortex image charges. Since only the amplitude of these signals is of interest, the shot-to-shot phase differences can be ignored.

III. THEORETICAL MODEL

The important quantities in the theoretical model of Moore and Saffman/Kida are the vorticity of the elliptical patch Ω and the strain rate e. The vorticity, which we define to be positive for our electron column, is given by $\Omega = ne/\epsilon_0 B$, where n is the electron density and B is the magnetic field strength. The theory assumes the vorticity is constant within the boundaries of the patch, whereas the density profile of our vortices is roughly Gaussian. To compare with theory, we assume that our vortex is comparable to a circular patch of radius R_v and density $N_L/\pi R_v^2$. Here $N_L = \int n\, dA/L$ is the number of electrons per unit length, L is the length of the column, $R_v = 1.5\int n|\mathbf{r}-\mathbf{R}_{cm}|dA/N_L$, $\mathbf{R}_{cm} = \int n\mathbf{r}\, dA/N_L$ is the position of the vortex center of mass, $n = n(r,\theta)$ is the density, which is determined from the pixel value at $\mathbf{r}=(r,\theta)$, and the integral is over the cross-sectional area of the device. The strain rate (or maximum rate of extension), e, is defined in a frame where the vortex center, R_{cm}, is at rest. In our case, this will be a frame rotating with angular velocity $\omega(R_{cm})$, where $\omega(r)=v(r)/r$ and v is the $\mathbf{E}\times\mathbf{B}$ drift velocity produced by the biased center wire (plus a small component due to the vortex image charges). In this frame the applied flow near R_{cm} is simple shear and $e = r(d\omega/dr)/2$ evaluated at $r = R_{cm}$. The strain rate is positive for positive center wire bias (i.e., the favorable shear case for the electron vortex). With these definitions, the key theoretical prediction can be simply stated: vortices with $e/\Omega < -(3-2\sqrt{2})/2 \cong -0.086$ will be dispersed, those with $e/\Omega > -0.086$ will remain. The theory assumes that in either case the vortex will remain an elliptical patch, although the axis ratio and orientation may change.

In order to make a valid comparison with theory, the system parameters should be adjusted to satisfy the two-dimensional (2-D) approximation. This requires that the axial transit time of the electrons be small compared to the time for motions in the $r-\theta$ plane. Two characteristic $r-\theta$ motions are the vortex spin around its own axis and its drift around the machine axis. Let γ_s denote the axial transit time over the vortex spin time and γ_d is the transit time over the drift time. For the parameters of these experiments $\gamma_s = 0.08$–0.4 and $\gamma_d = 0.003$–0.25, so the 2-D approximation is reasonable. End effects,[8] which can break the 2-D assumption, are negligible.

Finally, we note that the theory approximates the applied strain by employing a linear Taylor expansion around the center of the vortex. The next term in the expansion goes like $2R_v/R_{cm}$. In our experiments, $2R_v/R_{cm} = 0.25$, so the expansion is reasonable.

IV. QUALITATIVE BEHAVIOR OF A DISPERSING VORTEX

Examples of vortex evolution are shown in the phosphor screen images of Figs. 2–4. Except as noted, the screen bias is adjusted for each image, so that the full exposure is ob-

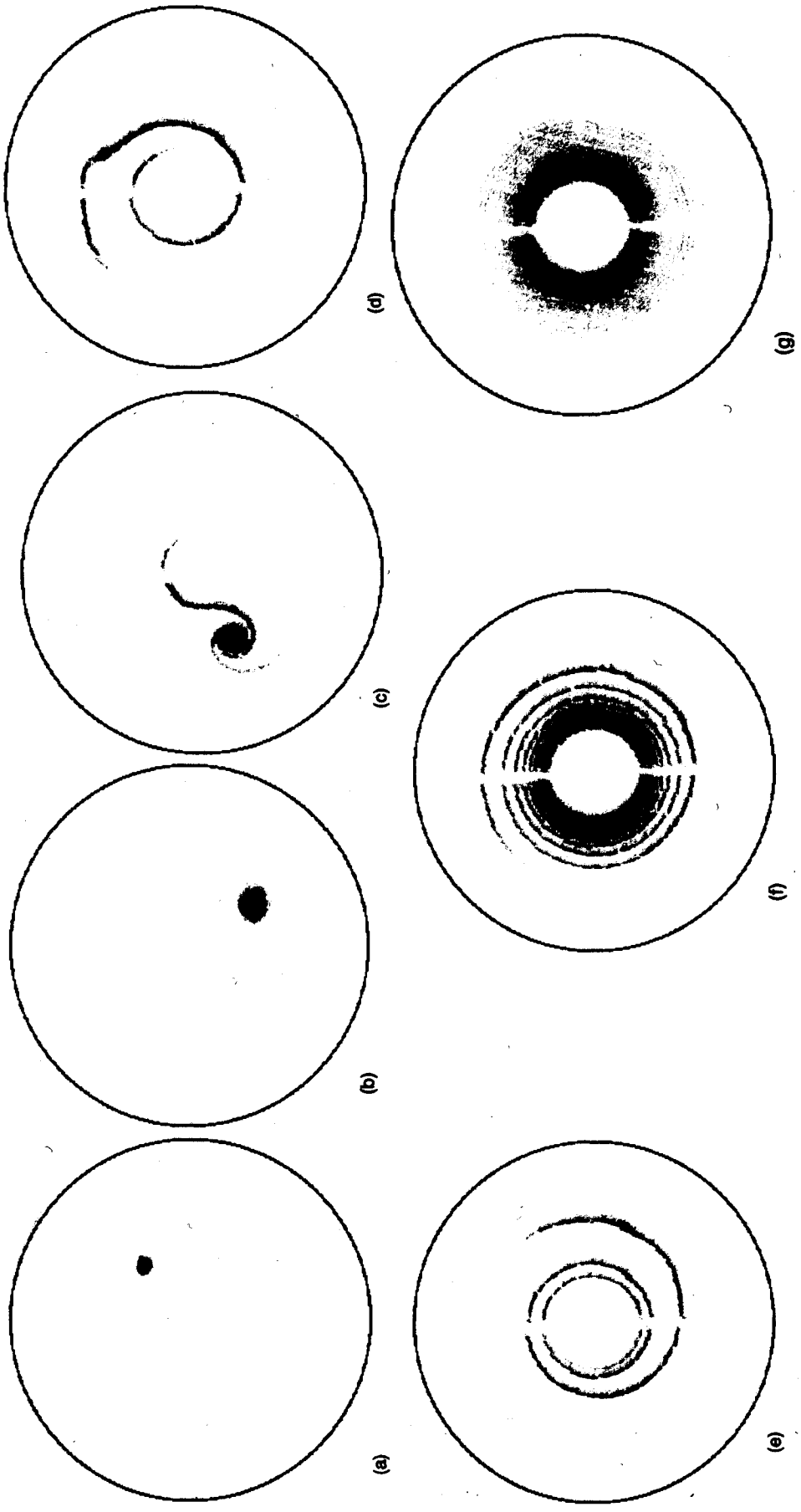

FIG. 2. Phosphor screen images of typical vortex evolution. Case 1 shows the emission of filamentary arms. Here, density $n = 2.08\times10^{7}$ cm^{-3}, central wire bias $\phi_{cw} = -78.1$ V, and $e/\Omega = -0.16$. (a) Initial injected vortex $t = 0$. (b) $t = 1.40$ μs. (c) $t = 2.70$ μs. (d) $t = 5.92$ μs. (e) $t = 9.02$ μs. (f) $t = 30.0$ μs. (g) $t = 110$ μs.

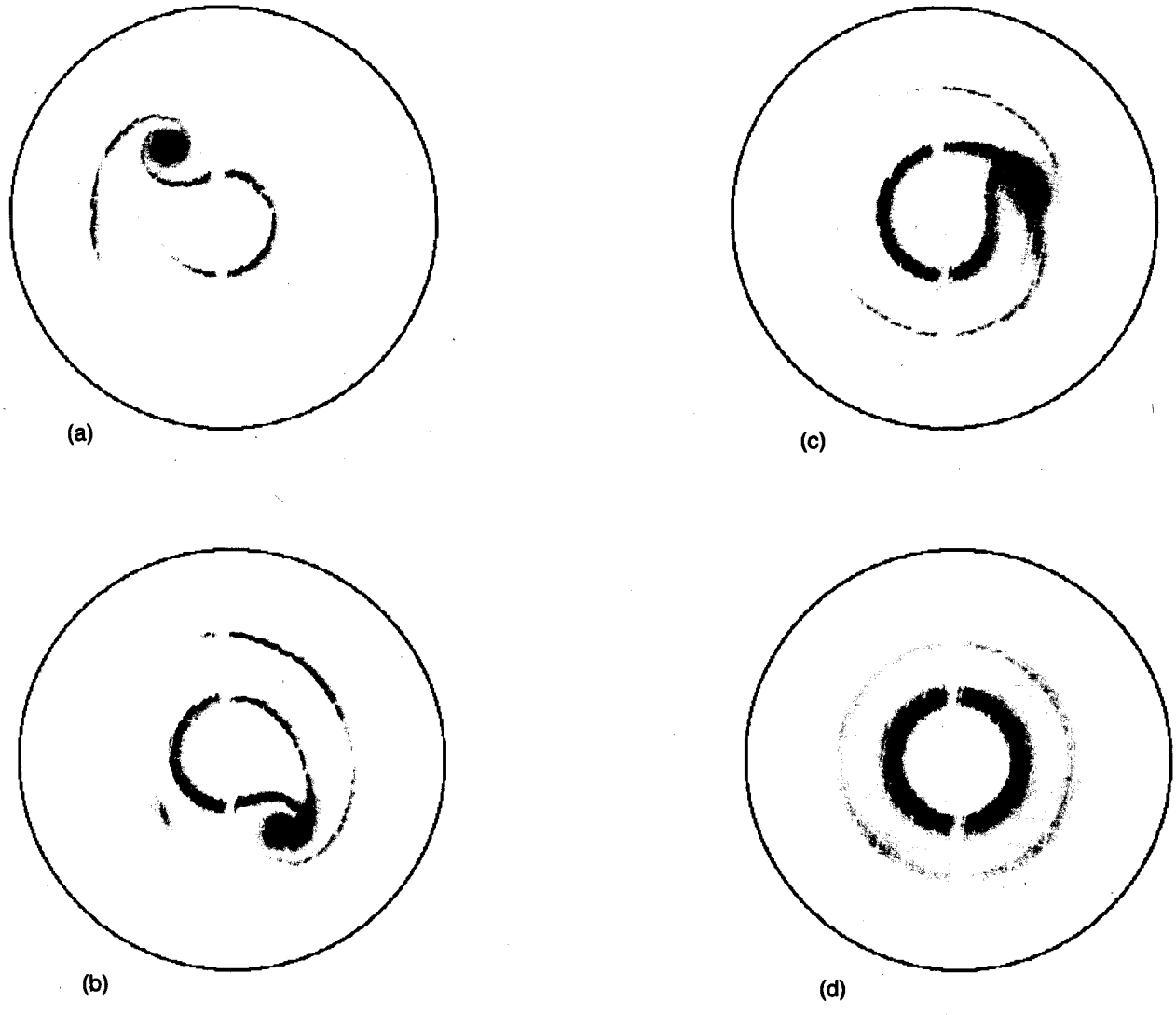

FIG. 3. Phosphor screen images of typical vortex evolution. Case 2 shows the entrainment of the filamentary arm. Here density $n = 2.08\times10^7$ cm^{-3}, central wire bias $\phi_{cw} = -69.5$ V, and $e/\Omega = -0.14$. (a) $t = 4.76$ μs. (b) $t = 8.06$ μs. (c) $t = 20.1$ μs. (d) $t = 135$ μs.

tained; if this were not done, the later images would be too dim to distinguish details. Also, we display negative images: darker parts of the image correspond to brighter parts of the phosphor screen and higher electron densities.

Figure 2(a) shows the initial vortex. For this case, $R_{cm} = 1.55$ cm and $R_v = 1.9$ mm. The calculated density n is 2.08×10^7 cm^{-3}, $\phi_{cw} = -78.1$ V, and $e/\Omega = -0.16$. The vortex center drifts clockwise around the central wire. As shown in Figs. 2(b) and 2(c), the vortex begins to disperse by emitting filamentary arms (these two images are overexposed, so that these low-density arms are visible). As time goes on, the arms continue to grow longer and wrap around the central wire [Figs. 2(d)–2(f)]. (Note: the vertical shadow in the images is produced by a bar that supports the central wire.) The filaments wind into a tighter and tighter spiral until the detail can no longer be resolved [Fig. 2(g)].

Figure 3 shows the evolution for a slightly smaller shear ($n = 2.08\times10^7$ cm^{-3}, $\phi_{cw} = -69.5$ V, $e/\Omega = -0.14$). The initial evolution is similar [Fig. 3(a)], but as the inner filamentary arm completes its first wrap around the central wire, it rejoins the vortex [Fig. 3(b); again (a)–(c) are overexposed to show detail]. The subsequent evolution shows turbulent variation from shot to shot; Fig. 3(c) is an average of eight shots. The turbulent dispersal of the vortex finally leads to a reproduceable end state [Fig. 3(d)]. Note that this end state is qualitatively different than the previous case [cf. Fig. 2(g)].

A final example of vortex evolution is shown in Fig. 4. Here the shear is stronger than in Fig. 2, and the density is lower: $n = 9.33\times10^6$ cm^{-3}, $\phi_{cw} = -138.8$ V, $e/\Omega = -0.64$. In this case, rather than emitting filamentary arms the initial vortex undergoes fission, splitting into two and then three smaller vortices before being smeared into a long filament. The winding process then proceeds as before. The end state exhibits a more uniform distribution of electrons than the previous cases. In general, this vortex fission occurs when e/Ω is large and negative (i.e., large adverse shear and low electron density).

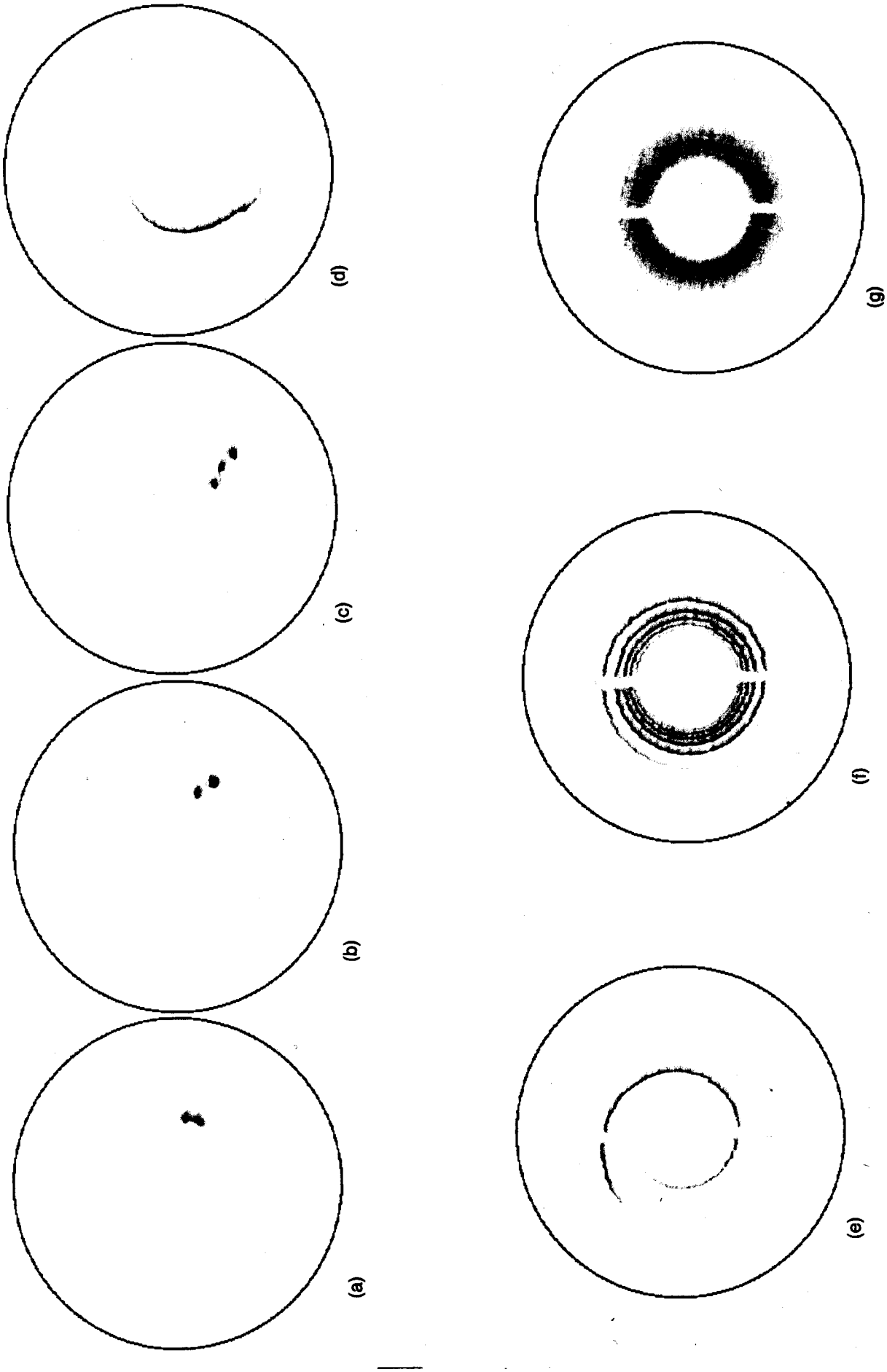

FIG. 4. Phosphor screen images of typical vortex evolution. Case 3 shows the breakup (fission) of the initial vortex. Vortex at $t = 0$ looks the same as in Fig. 2(a). Here, density $n = 9.33\times10^{6}$ cm^{-3}, central wire bias $\phi_{cw} = -138.8$ V, and $e/\Omega = -0.64$. (a) $t = 0.58$ μs. (b) $t = 0.68$ μs. (c) $t = 0.90$ μs. (d) $t = 1.70$ μs. (e) $t = 3.40$ μs. (f) $t = 13.6$ μs. (g) $t = 77.0$ μs.

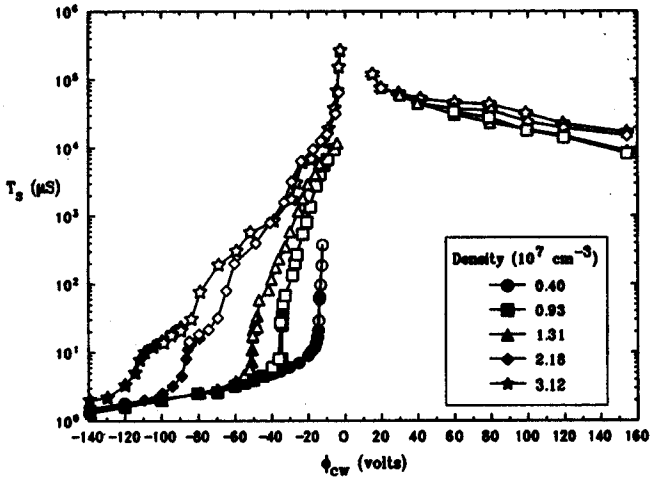

FIG. 5. Vortex shear time T_s versus central wire bias ϕ_{cw} with column density as a parameter.

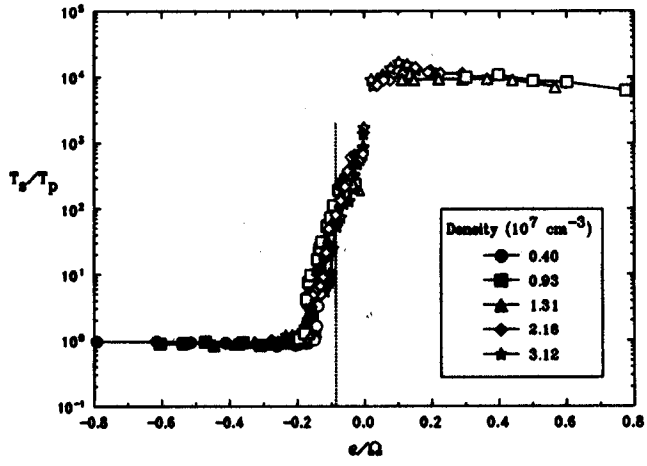

FIG. 6. The data of Fig. 5 plotted using the normalizations suggested by theory. Dashed vertical line shows the theoretical critical value.

V. MEASUREMENTS OF VORTEX LIFETIME

In order to quantify the shearing process, it is useful to define a quantity T_s, which measures the time it takes to shear (i.e., disperse) the vortex. The definition of T_s is chosen, so that the two methods available for monitoring the vortex dynamics (i.e., screen images and wall probe signals) give comparable values. For each image, the electron center of mass $\mathbf{R}_{cm}$ is calculated. Since the sector probe measures electrons within its 45° angular span, all pixel values within the span $\theta_{cm} \pm 22.5°$ are summed and divided by the sum at $t = 0$ (here θ_{cm} is the angle of the vector $\mathbf{R}_{cm}$). The shear time T_s is defined as the time when this ratio drops to 0.5 (i.e., when half the electrons have left the octant defined by $\theta_{cm} \pm 22.5°$). When the sector probe is used, T_s is defined as the time when the amplitude of the probe signal drops to half its initial value.

Data showing T_s versus the central wire bias ϕ_{cw} with column density (vorticity) as a parameter are presented in Fig. 5. The solid symbols are data points taken from screen images, and the open symbols are data points acquired with the wall probe. The qualitative features are consistent with expectations. When the shear is adverse and large (large negative values of ϕ_{cw}), the vortex is quickly dispersed (small T_s). As the shear is reduced (ϕ_{cw} is made less negative), the vortex lifetime increases. The shear value at which this increase occurs depends on the column's density (vorticity); more shear is required to disperse a stronger vortex. We also note that for favorable shear ($\phi_{cw} > 0$) the vortex lifetime is long and roughly independent of the value of ϕ_{cw}.

In Fig. 6, this data is replotted using scaled quantities. The shear time T_s has been scaled to the passive shear time T_p, which is the time it would take to shear a column with zero vorticity. We take this time to be $R_{cm}\theta_s/2eR_v$, where θ_s is the angular spread defining vortex dispersal (here taken as $\pi/4$ rad). On the abscissa is plotted the shear strength e divided by the vorticity Ω.

VI. DISCUSSION

The data of Fig. 5 now form one curve, showing that the scalings employed are the correct ones. The lifetime of a dispersed vortex is essentially T_p, and the parameter that determines the fate of the vortex is e/Ω. When e/Ω exceeds a critical value, the scaled vortex lifetime increases suddenly. The experimental critical value is slightly different for each of the cases considered, but the values do not exhibit any systematic dependence on density. The average experimental value is $(e/\Omega)_{crit} = -0.163 \pm 0.015$, in contrast with the theoretical value of -0.086. The vortex lifetime does not increase indefinitely at $(e/\Omega)_{crit}$. Rather, the lifetime jumps up abruptly by an order of magnitude and then follows a roughly exponential dependence on e/Ω. Thus, finite vortex lifetimes are obtained, even for applied shears substantially weaker than the critical value. The vortex lifetime reaches a roughly constant maximum value of $10^4 T_p$ for $e/\Omega > 0$.

The dependence of T_s/T_p on e/Ω for $e/\Omega > (e/\Omega)_{crit}$ can be explained as follows. The wall probe signal is qualitatively different for $(e/\Omega)_{crit} < e/\Omega < 0$ and $e/\Omega > 0$. For the first case, the signal is roughly constant in time, and then decreases abruptly, signaling that the vortex has been dispersed. Limited phosphor screen imaging corroborates this interpretation of the wall probe signal. For $e/\Omega > 0$, the probe signal decreases gradually until it is lost in the noise. The imaging data for this case shows that the vortex remains unsheared and that R_{cm} remains roughly constant. Both cases may be explained by the presence of a slow diffusive transport. When $(e/\Omega)_{crit} < e/\Omega < 0$, this transport causes the vortex density (and thus Ω) to decrease until e/Ω falls below $(e/\Omega)_{crit}$, at which point the vortex will be dispersed. For $e/\Omega > 0$, the shear is unable to disperse the vortex, regardless of the value of Ω, so the probe signal slowly decreases as electrons diffuse. The nature of this diffusion is unknown, but it is significantly faster than the transport that leads to particle loss. The time to lose half the electrons from the device is roughly ten seconds, whereas the maximum vortex lifetimes are on the order of 0.1 s.

We can offer no explanation for the factor-of-two dis-

crepancy between experimental and theoretical values for the critical e/Ω. One can identify several areas where the experiment departs from the theoretical model (e.g., Gaussian vortex profile, nonelliptical shape, finite second-order expansion terms) but a quantitative analysis of such effects is, to our knowledge, not available.

VII. CONCLUSIONS

We have studied the dynamics of a single vortex in an applied irrotational shear flow using a modified Malmberg–Penning trap. Time sequences of a dispersing vortex exhibit a variety of behaviors: vortex fission, filament emission, stretching, and entrainment, and turbulent diffusion. While none of these behaviors are included in the theory of Moore and Saffman/Kida, their theory correctly identifies the key dimensionless parameter e/Ω. However, the predicted critical value is roughly half of the experimental value. When e/Ω is less than the critical value, the vortex lifetime is the same as that of a zero vorticity patch. When e/Ω is above the critical value, the vortex lifetime increases dramatically and appears to be limited by a slow diffusive process that gradually weakens the vortex.

ACKNOWLEDGMENTS

The author gratefully acknowledges Dr. C. F. Driscoll's invaluable advice on the design of Malmberg–Penning traps; the assistance of Robin Chin, Douglas Copely, Adam Garrison, Alan Peel, Troy Reed, and Lee Talbert in the construction of the experimental device; seminal discussions of vortex dynamics with Dr. K. S. Fine; and Dr. Xiao-Pei Huang for pointing out an important error in the original manuscript.

This work was supported by Office of Naval Research (ONR) Grant No. N00014-89-J-1399.

[1]For a review, see P. G. Saffman and G. R. Baker, Annu. Rev. Fluid Mech. **11**, 95 (1979).

[2]D. W. Moore and P. G. Saffman, in *Aircraft Wake Turbulence*, edited by J. Olsen, A. Goldberg, and N. Rogers (Plenum, New York, 1971), pp. 339–354.

[3]S. Kida, J. Phys. Soc. Jpn. **50**, 3517 (1981).

[4]C. F. Driscoll and K. S. Fine, Phys. Fluids B **2**, 1359 (1990).

[5]In contrast, the finite viscosity and boundary effects present in most experiments in liquids appear to hamper efforts to compare theory and experiment. See, e.g., G. F. Carnevale, P. Cavazza, P. Orlandi, and R. Purini, Phys. Fluids A **3**, 1411 (1991); O. Cardoso, D. Marteau, and P. Tabeling, Phys. Rev. E. **49**, 454 (1994).

[6]K. S. Fine, C. F. Driscoll, J. H. Malmberg, and T. B. Mitchell, Phys. Rev. Lett. **67**, 588 (1991).

[7]J. H. Malmberg, C. F. Driscoll, B. Beck, D. L. Eggleston, J. Fajans, K. S. Fine, X.-P. Huang, and A. W. Hyatt, in *Non-Neutral Plasma Physics*, edited by C. W. Roberson and C. F. Driscoll (American Institute of Physics, New York, 1988), pp. 28–71.

[8]A. J. Peurrung and J. Fajans, Phys. Fluids B **5**, 4295 (1993).